Research Article

Cell Adherence Competition between Osteoblasts and Fibroblasts on Various Materials Influences the Establishment of Osseointegration

Miho Tamai[1, 2], Kenichi Harimoto[1], Noriyuki Nagaoka[3], Kumiko Yoshihara[4, 5], Yasuhiro Yoshida[2], Yoh-ichi Tagawa[1*]

[1]School of Life Science and Technology, Tokyo Institute of Technology, Yokohama, Japan

[2]Faculty of Dental Medicine, Hokkaido University, Sapporo, Japan

[3]Okayama University Dental School, Advanced Research of Center for Oral and Craniofacial Science, Okayama, Japan

[4]Okayama University Graduate School of Medicine, Dentistry and Pharmaceutical Sciences, Okayama, Japan

[5]National Institute of Advanced Industrial Science and Technology (AIST), Health and Medical Research Institute, Kagawa, Japan

*Corresponding author: Yoh-ichi Tagawa, School of Life Science and Technology, Tokyo Institute of Technology, 4259 B51, Nagatsuta-cho, Midori-ku, Yokohama, 226-8501, Japan, Tel: 81-45-924-5791; Fax: 81-45-924-5809

Citation: Miho Tamai, Kenichi Harimoto, Noriyuki Nagaoka, Kumiko Yoshihara, Yasuhiro Yoshida, Yoh-ichi Tagawa. Cell Adherence Competition between Osteoblasts and Fibroblasts on Various Materials Influences the Establishment of Osseointegration. Archives of Clinical and Biomedical Research 5 (2021): 650-663.

Abstract

Osseointegration is a key factor in determining the success of a prosthetic implant. Titanium and its alloys are widely used as implantable materials because of good adaptation and connection to bone tissues, known as osseointegration. We focused on the invasion of fibrous tissue into the bone tissue–material interface and hypothesized that there might be competition for cell adhesion between osteoblasts and fibroblasts on the material surface.

In this study, we established a cell competition model in a co-culture of osteoblasts and fibroblasts under shear stress conditions to elucidate fibroblast-associated failure of osseointegration after implantation. The osteoblasts adhere better on titanium than fibroblasts under shear stress conditions. The alkaline phosphatase–positive cells were increased when osteoblasts were co-cultured with fibroblasts, suggesting that the small population of fibroblasts promotes osteoblast differentiation through the production of extracellular matrices including type I collagen. Cell adhesion competition created a balance of osteoblasts and fibroblasts on the implant material surface in the initial stage of osseointegration resulting in a high osseointegration ratio. These results show

that fibroblasts are able to both inhibit osseointegration and help adhesion and differentiation of osteoblasts by producing type I collagen.

Keywords: Osteoblast; Fibroblast; Osseointegra-tion; Cell adhesion; Cell competition

1. Introduction

Osseointegration is a key factor in determining the success of a prosthetic implant and fibrous tissue can invade the interface between bone and materials when osseointegration fails [1]. Fibroblasts mainly contribute to the formation of fibrous tissue and repress the proliferation of osteoblasts and its mineralization in co-cultures of osteoblasts and fibroblasts [2]. Since osseointegration is the stable adherence state between the implant material and bone [3-5], the selection of implant materials affects clinical success. Titanium is known to be an implant material that accelerates osseointegration. Titanium is a biocompatible material with high corrosion resistance due to its thin protective oxide (TiO_2 or titania) layer which spontaneously develops on its surface when exposed to air [6]. For this reason, titanium and its alloys are widely used in biomedical devices and prosthetic components, such as orthopedic joints, dental implants, and artificial vascular stents [7-9]. Based on clinical experience, titanium is the most superior for osseointegration formation compared to other materials; however, the biological mechanism of osseointegration between titanium implants and bone is not well understood [10].

It has been reported that cell adherence levels are dependent on the materials used through a comparison of alumina and zirconia to titanium; however, the effect of surface roughness was not considered in this comparison [11]. Micro- or nanoscale surface roughness affects osteoblast behavior and the adherence of the implant with the bone surface [12-14]. It is important to consider the roughness of each

material surface in order to compare how different materials affect the mechanism of osseointegration. Furthermore, the study of material sciences along with biomechanical sciences helps to optimize the design and material concepts for surgical implants [15].

We aimed to elucidate the mechanism of biocompatibility of implant materials by investigating 1) how shear stress affects cell adhesion, proliferation, and differentiation in the *in vitro* co-culture model of fibroblasts and osteoblasts and 2) how different extracellular matrices affect cell activity. In order to investigate the process of osseointegration formation, we established a cell competition model in a co-culture of osteoblasts and fibroblasts using two types of fluorescent proteins and applying shear stress. This model is useful for clarifying the mechanism of fibroblast-associated failure of osseointegration after implantation.

2. Materials and Methods

2.1 Materials preparation

Unblemished glass discs (15-mm diameter, 1-mm thickness, B270-superwhite, Hiraoka Special Glass Mfg, Osaka, Japan) were cleaned first with an alkali detergent, followed by distilled water, and isopropyl alcohol by ultrasonic rinsing. Subsequently, Ti, Al_2O_3, ZrO_2, and Au films were deposited on the cleaned glass discs by an electron beam evaporator (BMC-1100, Shincron, Yokohama, Japan) up to a film thickness (Table 1).

To improve the adhesion of gold to the glass disc, a 1-nm thick Cr layer was first deposited. The resulting film thickness was monitored by a quartz balance installed inside the evaporation chamber, which was adjusted to an accuracy of approximately 10%. The deposited coated glass discs were additionally checked using a field-emission-gun scanning electron microscope (FE-SEM; JSM-6701F, JEOL, Tokyo, Japan), operated at an accelerating voltage of 5 kV, and subsequently using a transmission electron microscope

(TEM; JEM-2100, JEOL, Tokyo, Japan) operated at an accelerating voltage of 200 kV. Before FE-SEM examination, the $Al_2O_3^-$ and ZrO_2^- deposited glass discs were coated with a 3-nm osmium layer by using an osmium coater (Meiwa Fosis Neoc-STB, Tokyo, Japan).

Material	Film thickness
Ti	40 nm (10%)
Al_2O_3	50 nm (10%)
ZrO_2	50 nm (10%)
Cr + Au	Cr (lower layer) 1 nm (10%), Au (upper layer) 49 nm (10%)

Table 1: The thickness of film coated on a glass disc.

2.2 Cell culture

Cells of the mouse osteoblast-like cell line MC3T3-E1 and mouse fibroblast cell line NIH3T3 (both cell lines were donated from RIKEN Cell Bank, Ibaraki, Japan), were cultured in an α-modified essential medium (α-MEM) supplemented with antibiotics (penicillin/streptomycin; Invitrogen, Tokyo, Japan), 4 mM L-glutamine (Invitrogen), and 10% fetal bovine serum (FBS; Nichirei Biosciences, Tokyo, Japan) in 5% CO_2 at 37°C. The cells were subcultured by treatment with 0.05% trypsin (Wako, Osaka, Japan) and 20 μM ethylenediaminetetraacetic acid (EDTA; Invitrogen).

The conditioned medium is the culture supernatant produced by NIH3T3 culturing for 24 hours in serum-free medium.

2.3 Establishment of cells carrying DsRed2 or AcGFP expression vector

The expression vectors of *DsRed2* and *AcGFP fluorescence protein* genes, *pCAGDsRed2-neo* and *pCAGAcGFP-neo*, respectively, were regulated by the *CAG promoter* (Ryu et al, 2012) [16]. These expression vectors were introduced in to MC3T3- E1 or NIH3T3 cells by the electroporation method as described previously (Harimoto et al, 2012) [17]. Briefly, 1 x 10^7 cells/0.9 ml in PBS of MC3T3-E1 or NIH3T3 cells was mixed with 25 μg of linearized *pCAGDsRed2-neo*/Eco RI or *pCAGAcGFP-neo*/Eco RI, respectively, and were transfected by the electroporation method. After electroporation, cells were seeded onto 100-mm diameter gelatin-coated plastic dishes. The culture medium containing 400 μg/ml or 1 mg/ml G418 was changed a day after the electroporation of MC3T3-E1 or NIH3T3 cells, respectively. G418-resistant colonies were picked up. The clones were maintained as were the parental cells. The expression of those clones was confirmed by the flow cytometer (Beckman Coulter, CA), and then finally each clone with the strongest expression of the *DsRed2* or *AcGFP* gene was established as the MC3T3-E1^{Red} or NIH3T3^{Green} cell-line, respectively.

2.4 Osteoblast differentiation

To test the differentiation of osteoblasts, a concentration of 1×10^5 cells/disc was seeded in each well of a 24-well plate, with each well containing one disc coated with one of the four substrates tested. The osteoblasts were incubated at 37°C in 5% CO_2 atmosphere. After 24 h, the media were changed and the cells were incubated in culture medium that was additionally supplemented with 50 μg/ml L-ascorbic acid (Wako) and 10 mM β- glycerophosphate (Wako). The day of changing to this specific medium was considered as day zero. The medium was changed twice a week. After 2 and 4 weeks, the cultures were

stained with alkaline phosphatase (ALP) and alizarin red for mineralized nodules.

2.5 Immunohistochemical analysis

Cells were cultured on each disc for 24 h and were fixed with 4% paraformaldehyde/PBS for 10 min and then permeabilized with 0.1% Triton X for 5 min at room temperature. The fixed samples were incubated in Blocking One (Nacalai tesque, Kyoto, Japan) for 30 min, then incubated with the primary antibody for 2 h and the secondary antibody for 1 h at room temperature. The following antibodies were used: mouse anti-vinculin (1:200, Sigma-Aldrich, STL) and Alexa Fluor 594 donkey anti-mouse IgG (1:2000, Invitrogen). For F-actin and nuclear staining, cells were incubated for 30 min with Actin Stain^{TM} 488 Fluorescent Phalloidin (Cytoskeleton, Denver, CO) and DAPI (4, 6-diamidino-2-phenylindole). The samples were mounted in Prolong Gold fluorescent mounting medium and observed using a fluorescence microscope (Olympus, Tokyo, Japan).

2.6 Alkaline phosphatase and Alizarin Red S staining

Alkaline phosphatase and Alizarin Red S staining were carried out as described previously (Harimoto et al, 2012) [17]. Briefly, after washing, the culture discs were incubated for 30 min in a solution of alkaline phosphatase substrate produced using an Alkaline Phosphatase Substrate Kit III (Vector Laboratories, Burlingame, CA). After washing, the cells were fixed with ethanol and stained with 1% Alizarin Red S (Wako) in order to visualize the calcium deposits on cells. Alizarin Red S binds selectively to calcium; the stained material appears dark red.

2.7 Cell adhesion assay

Each of the three discs was fixed in 6-well culture plates. Cells were seeded at 1×10^6 cells/well in α-MEM with 10% FBS. The plates were placed on the shaker with or without up and down shaking. At predetermined

time points, the cells were rinsed three times with PBS to remove non-adhered cells. The cell number was analyzed by image processing software (ImageJ, open source, public domain) according to the fluorescent photographs taken at random points of each disc.

2.8 Morphological observation of the cells

MC3T3-E1^{Red} were seeded on each disc at a density of 1×10^4 cells/well in α-MEM supplemented with 10% FBS; they were cultured under standard culture conditions for 24 h. The samples were then washed with PBS. The morphology of the adhered cells was observed using an inverted fluorescence microscope (Olympus).

2.9 RNA extraction and reverse transcription-polymerase chain reaction analysis

RNA preparation and RT-PCR were carried out as described previously [18]. Briefly, total RNA was prepared from the cells by the acid guanidinium isothiocyanate-phenol-chloroform-isoamyl alcohol method. Total RNA samples were reverse transcribed using a Superscript II first-strand synthesis system (Invitrogen) with an oligo (dT) primer (Invitrogen). PCR was performed using Ex Taq DNA polymerase (Invitrogen). Primer sequences are listed in supplemental table 1.

3. Results

3.1 Unique adhesion morphology of MC3T3-E1 on titanium-evaporated discs

Four representative material surfaces namely titanium, alumina, zirconia, and gold, which were almost the same roughness by their evaporation, were used in order to compare how different materials affect osseointegration. MC3T3-E1, a pre-osteoblast cell line, was cultured on material-evaporated discs of titanium, alumina, zirconia, and gold, and within 24 h had spread to completely cover the discs. Actin fibers could be clearly observed in the cells on all types of discs by staining with phalloidin, which specifically binds to a

cytoskeleton protein F-actin (Figure 1A).

The cells spread significantly wider on titanium than on alumina or gold 24 h after seeding (Figure 1B). The number of focal adhesions observed at the terminus of the actin fibers by anti-vinculin antibody staining was dependent on the kind of material (Figure 1A), and the number of focal adhesions was significantly greater on titanium than on other materials (Figure 1C). Furthermore, to observe cell adhesion behavior along the time course, the *pCAG- DsRed2-neo* expression vector was introduced into the osteoblast cell line MC3T3-E1, and a red fluorescence osteoblast cell line MC3T3-E1[Red] was cloned and established. The fluorescence observation under G-excitation revealed that MC3T3-E1[Red] cells adhered and spread on all four discs tested. Serum-dependent cell adhesion was investigated in the early phase, 0.5 and 1.0 h after seeding onto each disc. Most of the cells started to spread and exhibited filopodia and lamellipodia by 0.5 h on titanium but not on other materials (Figure 1D), and the number of adhered cells on titanium was highest at 0.5 h (Figure 1E). However, the cells spread on all discs by 1.0 h, and the number of adhered cells achieved the same level at 1.0 h (Figure 1F). These results suggest that MC3T3-E1[Red] can attach and spread more easily on titanium in the medium containing serum than on other materials. These tests demonstrate that the identity of a material and its natural attributes play a crucial role in the very early stages of cell adhesion, even in the presence of serum components.

3.2 NIH3T3[Green] achieved greater adhesion than MC3T3-E1[Red] on zirconia, alumina, and gold discs, but not on titanium discs

The effect of fibroblasts on bone formation after implantation *in vivo* is also an important factor. To construct an *in vitro* model of bone formation, MC3T3-E1 cells and NIH3T3 fibroblasts were co-cultured on each disc. To discriminate MC3T3-E1 and

NIH3T3, the *pCAG-AcGFP-neo* expression vector was introduced into the fibroblast cell line NIH3T3, and the green fluorescence osteoblast cell line NIH3T3[Green] was cloned and established. The number of adhered cells for each cell line was counted by data gathered using the ImageJ system from fluorescent photographs. In order to analyze cell adhesion under competitive conditions, 5×10^5 cells of MC3T3-E1[Red] and NIH3T3[Green] were simultaneously seeded on each disc, and the adhered cell number for each cell line was compared on each disc after 6 h. In the case of single cultures, the number of MC3T3- E1[Red] on gold was higher than on titanium (Sup Figure 1A), and the number of NIH3T3[Green] on gold was higher than other materials (Sup Figure 1B). On the other hand, MC3T3-E1[Red] and NIH3T3[Green] could be easily differentiated in the culture on each disc (Figure 2A). The cell count of NIH3T3[Green] was higher than that of MC3T3-E1[Red] on zirconia, alumina, and gold discs, but there was no significant difference in titanium discs (Figure 2B).

3.3 Titanium has a much higher MC3T3-E1[Red] attachment potential under shear stress conditions than other materials

In order to investigate the potential of cell adhesion in a mimicked *in vivo* environment on each disc surface, we put the culture system on the shaker to examine the effects of shear stress during the cell adhesion step. MC3T3-E1[Red] and NIH3T3[Green] (1×10^6 cells each) were seeded on each disc, and the adhered cell number was compared amongst each disc after 6 h culturing with shear stress. The adhered cell number of MC3T3-E1[Red] on the titanium disc was significantly higher than other discs, but the adhered cell number of NIH3T3[Green] was not different among the discs (Sup Figure 1C and D). Next, a mixture of 5×10^5 cells each of MC3T3-E1[Red] and NIH3T3[Green] were seeded on each disc and cultured on a shaker. The fluorescence photographs taken at 6 h after seeding show that the number of MC3T3-E1[Red] was higher than NIH3T3[Green] on titanium but this relationship was reversed on gold

discs (Figure 2C). The cell number analysis from the photographs also indicated that MC3T3-E1[red] adhered more to titanium discs and less on gold discs than NIH3T3[Green], but there was no significant difference between the two cell lines on zirconia or alumina discs (Figure 2D).

3.4 Type I collagen is important for MC3T3-E1[Red] to outcompete NIH3T3[Green] in the adhesion stage

5×10^5 cells of MC3T3-E1[Red] were seeded on each disc in the conditioned medium. The cell number was counted 6 h after seeding with MC3T3-E1[Red]. There was no difference in the number of adhering cells on titanium between the 10% FBS–medium and the conditioned medium. Cell numbers on zirconia and alumina with the conditioned medium was higher than the number with the FBS medium (Fig. 3A).

In order to clarify the matrix molecules affecting adhesion competition under shear stress conditions, we coated the cell culture plate with 50 μg/ml matrix molecules and cultured on a shaker during the cell adhesion step. Fibronectin, collagen type 1, collagen type 4, laminin, vitronectin, and osteopontin were used as matrix molecules for the experiments. MC3T3-E1[Red] and NIH3T3[Green] (5×105 cells each) were seeded simultaneously on each matrix molecule. The cell number was counted after 6 hours. The number of MC3T3-E1[Red] was significantly higher than NIH3T3[Green] on collagen type I (Fig. 3B). To confirm whether collagen type I was the key matrix molecule, gene expression was analyzed for *collagen type I* and *integrin subunit* types which are cell adhesion molecules. However, there was no significant difference in *collagen I* and *fibronectin* expression

between MC3T3-E1[Red] and NIH3T3[Green], even when cultured on discs of a different material (Fig. 3C and D). On the other hand, MC3T3-E1[Red] expressed *integrin α1 subunit*, which is known as a collagen 1 receptor, stronger than NIH3T3[Green].

Next, we investigated the cell adhesion competition on the four kinds of discs coated with collagen type I. Each disc was coated with 50 μg/ml collagen type I solution overnight. MC3T3-E1[Red] and NIH3T3[Green] (5×10^5 cells each) were seeded simultaneously on each of the collagen type I–coated discs and cultured on a shaker. The number of MC3T3-E1[Red] was higher than the number of NIH3T3[Green] on any kind of disc coated with collagen type I, but the MC3T3-E1[Red] adhesion number was the highest on titanium discs (Fig. 3E). The results suggested that type I collagen may be the key protein in cell adhesion competition between MC3T3-E1[Red] and NIH3T3[Green].

3.5 The effect of NIH3T3[Green] on MC3T3-E1[Red] differentiation

In the mixture of the MC3T3-E1[Red] and NIH3T3[Green] (ratio, 1:9, 5:5, and 9:1), MC3T3- E1[Red] cells were differentiated to osteoblasts on titanium discs by the addition of 50 μg/ml L-ascorbic acid, 10 mM β-glycerophosphate, and 100 ng/ml BMP-2. Two weeks after induction, MC3T3-E1[Red] cells could be differentiated to alkaline phosphatase-positive cells and NIH3T3[Green] strongly promoted osteogenic differentiation (Figure 4A). Four weeks after induction, calcium deposition could be observed by Alizarin Red S staining. NIH3T3[Green] slightly promoted mineralization (Figure 4B).
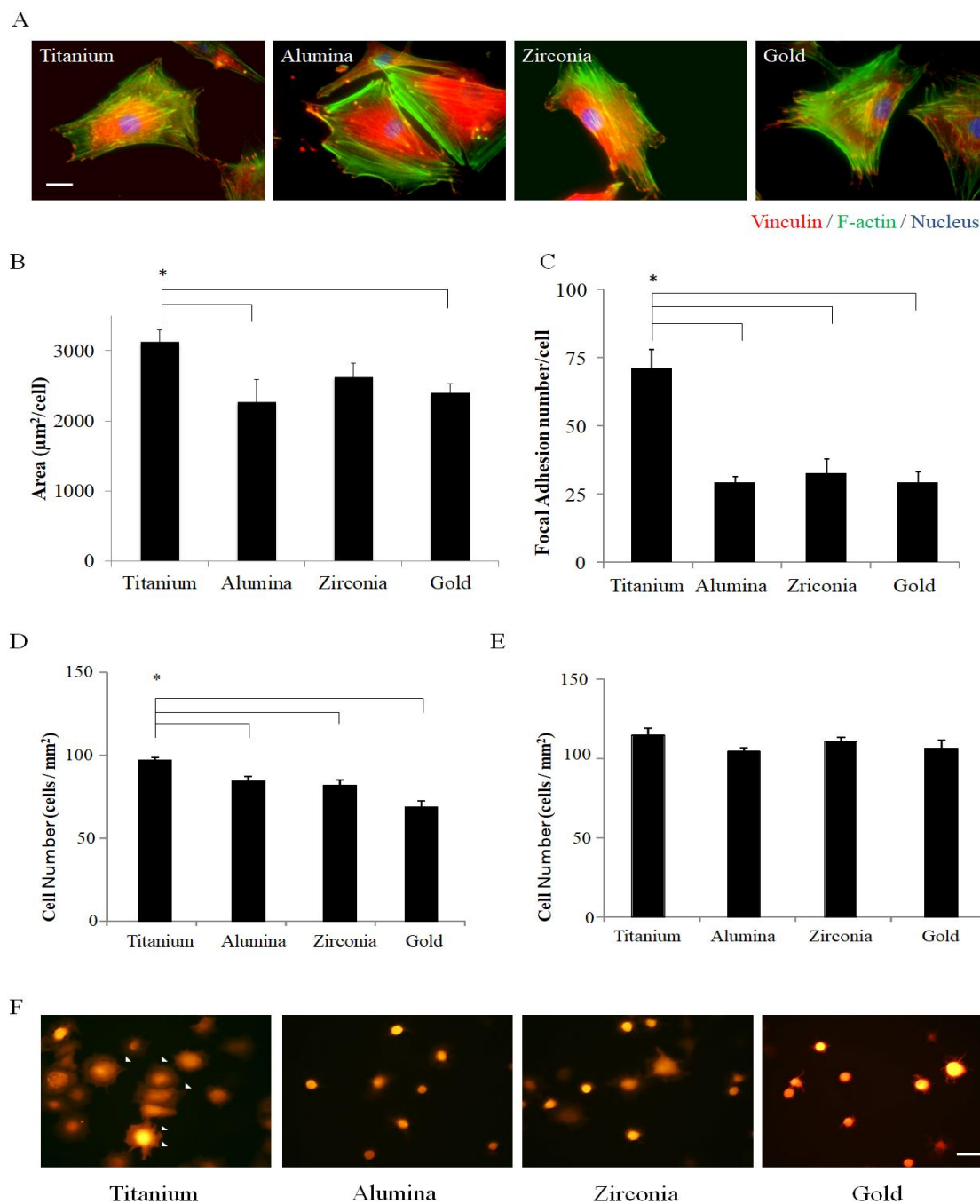
Figure 1: Cell adhesion property on each material. (A) MC3T3-E1 cells cultured on each disc for 24 h were fixed and subsequent immune fluorescence staining was performed using an anti-vinculin antibody, phalloidin, and DAPI. Vinculin was stained red, F-actin was stained green, and the nucleus was stained blue. Fluorescent pictures were taken and the representative morphology of a cell on each disc is shown; (B) Average aspects of MC3T3-E1 were analyzed from each fluorescent picture and indicated in the graph. (n=6); (C) The graph shows the focal adhesion number of MC3T3-E1 on each disc 24 h after cells were seeded; (n=8) (D, E) MC3T3-E1red cells were seeded at 5×10^5 cells/well containing three discs per well. The graphs show the number of adhered cells on each disc after 30 min (D) and 1 h (E). (F) The fluorescent picture shows the MC3T3-E1red adhesion on each disc after 30 min. White arrows indicate the spreading cells on discs. Data are expressed as the mean ± SEM. Analysis of variance (ANOVA) was performed, and significant differences between discs were determined using the Tukey test (*: P < 0.05).
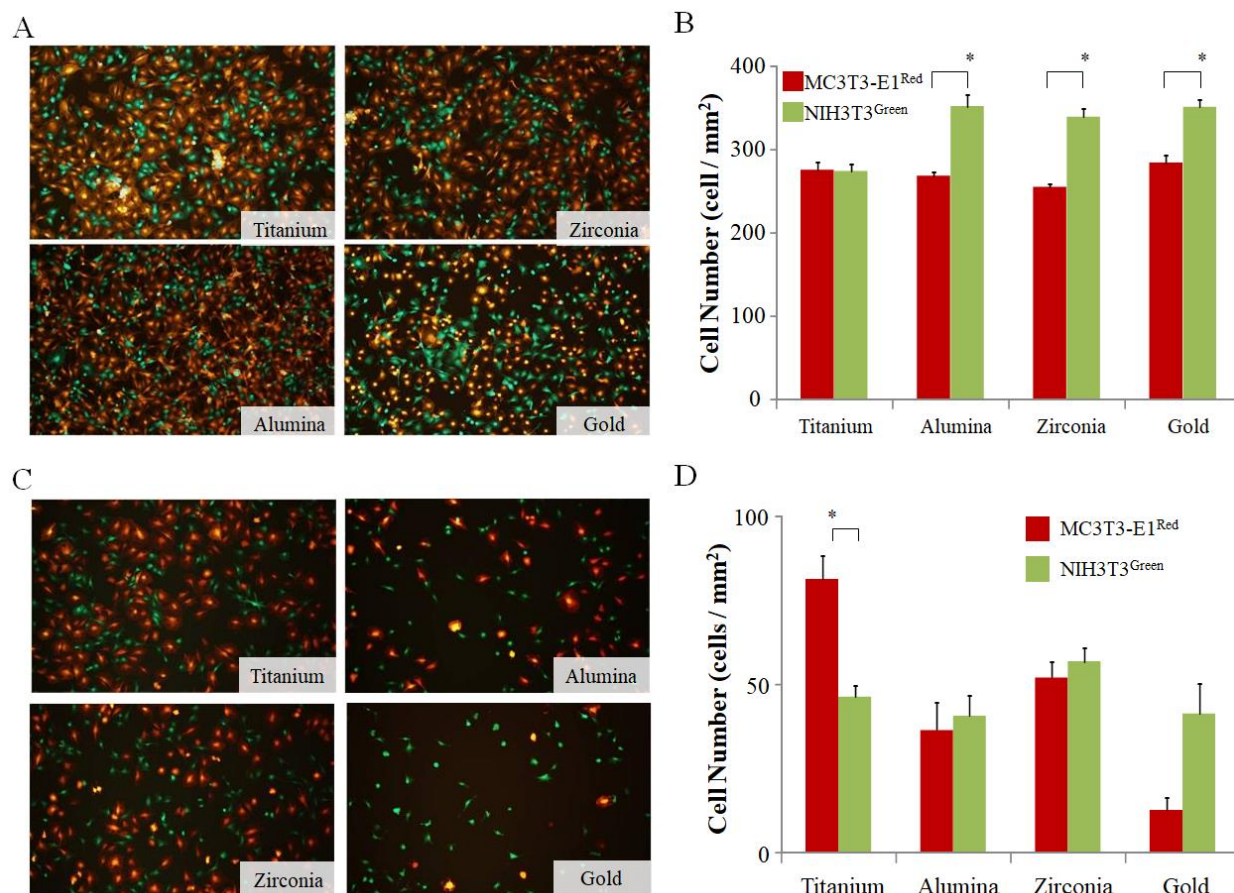
Figure 2: Cell adhesion competition without and with shear stress conditions. (A) MC3T3-E1[red] cells and NIH3T3[green] cells were seeded simultaneously at 5×10^5 cells/well to the same well with three discs. The fluorescent pictures were taken after 6h and show the MC3T3-E1[red] and NIH3T3[green] adhesion on each disc surface after 6 h without shear stress; (B) The graphs show the number of adhered MC3T3-E1[red] cells and NIH3T3[green] cells analyzed from the fluorescent pictures. Red bars indicate MC3T3-E1[red], and green bars indicate NIH3T3[green]; (C) MC3T3-E1[red] cells and NIH3T3[green] cells were seeded simultaneously at 5×10^5 cells/well to the same well with three discs, and they were cultured on a shaker with up-down shaking. The fluorescent pictures were taken after 6 h and show the MC3T3-E1[red] and NIH3T3[green] adhesion on each disc surface after 6 h; (D) The graphs show the number of adhered MC3T3-E1[red] cells and NIH3T3[green] cells analyzed from the fluorescent pictures. Red bars indicate MC3T3-E1[red], and green bars indicate NIH3T3[green]. Data are expressed as the mean ± SEM (n=3). Analysis of variance (ANOVA) was performed, and significant differences between discs were determined using the Tukey test (*: $P < 0.05$)
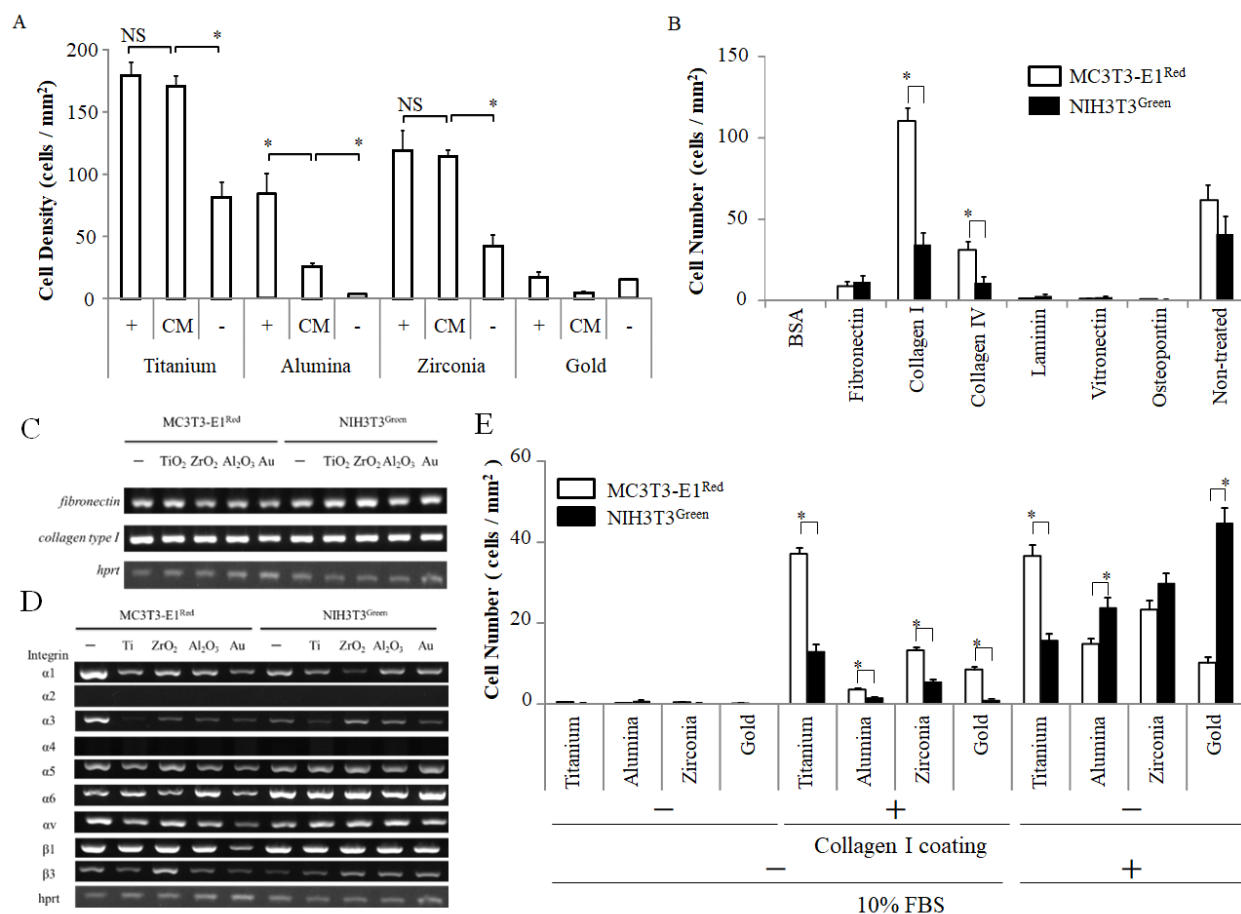
Figure 3: Cell adhesion on matrix proteins. (A) MC3T3-E1^{red} cells were seeded at 1×10^6 cells/well in a well with three discs, and they were cultured on a shaker with up-down shaking. The culture mediums used were serum-containing medium (+), serum-free medium (-), and conditioned medium (CM). The graphs show the number of adhered MC3T3-E1^{red} cells; (B) MC3T3-E1^{red} cells and NIH3T3^{green} cells were seeded simultaneously at 5×10^5 cells/well to the same well coated by each matrix protein, and they were cultured on a shaker with up-down shaking. (C, D) The gene expression of MC3T3-E1^{red} and NIH3T3^{green} cultured on each disc for 24 days was examined by RT-PCR. The gene related to matrix protein; (C) and the gene related to *integrin subunits;* (D) is indicated; (E) MC3T3-E1^{red} cells and NIH3T3^{green} cells were seeded simultaneously at 5×10^5 cells/well containing type I collagen-coated discs, and they were cultured in serum-free medium on a shaker with up-down shaking. The graphs show the number of adhered MC3T3-E1^{red} cells and NIH3T3^{green} cells after 6 h in culture. Data are expressed as the mean ± SEM (n=3). Analysis of variance (ANOVA) was performed, and significant differences between discs were determined using the Tukey test (*: $P < 0.05$). Red bars indicate MC3T3-E1^{red}, and green bars indicate NIH3T3^{green}.
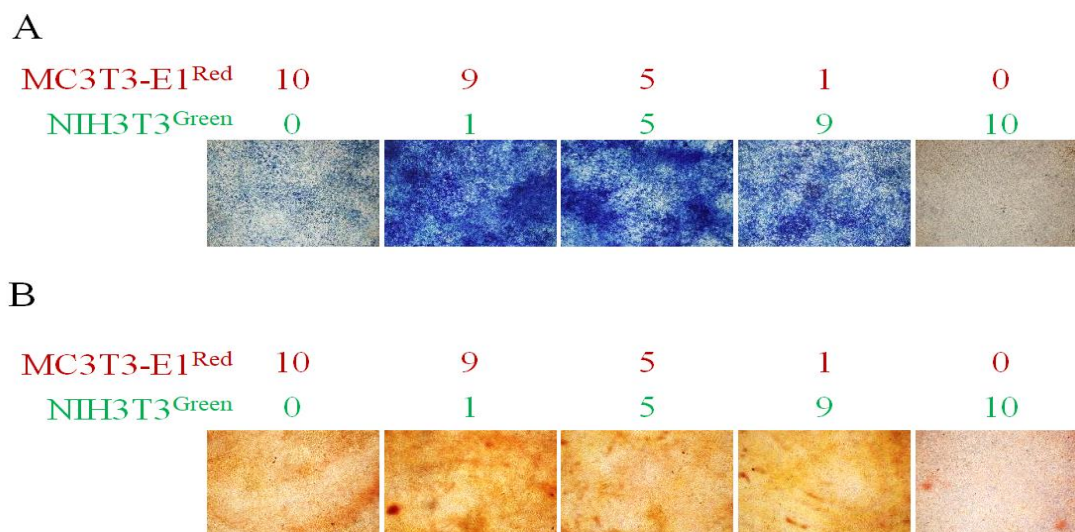
Figure 4: Osteoblast differentiation and mineralization. The MC3T3-E1[red] cells and NIH3T3[green] cells were mixed in the indicated ratios and cultured on a titanium disc in differentiation-inducing medium. (A) ALP staining was performed after 2 weeks. Osteoblast differentiation was observed by staining ALP- positive cells (blue); (B) Alizarin Red S staining was performed after 4 weeks. Osteoblast mineralization was observed in the red region indicating calcium deposition.

4. Discussion

Since osseointegration is affected by the roughness of a material's surface, the surfaces of the materials used in this study were adjusted to the same level of roughness. Electron- beam evaporation is a powerful technique to prepare well-crystallized oxide films with a high deposition rate and controlled stoichiometry by adjusting conditions such as the substrate temperature, oxygen gas pressure, and evaporation rate [19, 20]. The difference in the roughness of the evaporated glass discs we used in this study was not significant and was in the 2 nm (Ra) range; the effects of roughness could be practically ignored. These discs were used to investigate whether the attachment of cells depended on the surface nature of the materials. Broad and rapid cell spreading on titanium was shown in this study (Figure 1); on the other hand, the number of adhered cells was higher on gold discs than on titanium discs (Sup Figure 1A and B). Because fibroblast invasion led to the failure of complete osseointegration of the implant therapy [21-23], we focused on the existence of fibroblasts. Because the titanium surface was

thought to have an advantage in the early stage MC3T3-E1[Red] adhesion competition between osteoblasts and fibroblasts, we investigated the adherence competition between NIH3T3[Green] and MC3T3-E1[Red] on each disc. The number of adhered MC3T3-E1[Red] was as same as the number of NIH3T3[Green] only on titanium but was lower on others. This suggests that the titanium disc is more suited for osteoblast attachment than for fibroblasts.

Mechanical loading also plays an important role in skeletal development and the maintenance of the skeletal architectural integrity [24]. The primary and clonal osteoblast-like cells responded to shear stress with increased cell proliferation and differentiation [25, 26]. Low fluid shear stress plays an important role in the activation of many factors including osteoblasts and intracellular calcium, nitric oxide, and other cell messengers [26]. In order to verify the potential of the titanium disc for osteoblast attachment, the same experiments were repeated with the addition of shear stress that would be expected in an *in vivo* environment.

In the results of a single type of cell seeding (Sup Figure 1C and D), although the attached number of NIH3T3^{Green} was decreased on all discs, the attached number of MC3T3-E1^{Red} was conserved on titanium discs but not on others. When the cell mixture of NIH3T3^{Green} and MC3T3-E1^{Red} seeded on each material disc under shear stress conditions, MC3T3-E1^{Red} mainly occupied the titanium discs and not others (Figure 2). These results indicate that osteoblasts can outcompete fibroblasts in cell attachment competition on the titanium surface. This makes titanium unique for osseointegration, as osteoblasts rapidly and tightly adhere to the surface as compared to the other substrate materials tested.

In order to answer the question of why there is a difference between MC3T3-E1^{Red} and NIH3T3^{Green} attachment on titanium, the gene expression of *integrin subunit* type, which is a cell adhesion molecule, was investigated. There was no significant difference between MC3T3-E1^{Red} and NIH3T3^{Green}, and no difference among the discs (Figure D). These results mean that the difference in cell attachment is not due to the cellular factors. It has been shown that the osteoblast compatibility of materials depends on serum protein absorbability [17] and the adsorption of extracellular matrix proteins on the material surface has been demonstrated to mediate cell adhesion. Therefore we next tried to test which matrix protein is suited for MC3T3-E1^{Red} attachment. Six kinds of matrix proteins that exist *in vivo* in nature were tested. According to the results, collagen type I is the best matrix protein (Figure 3B and E). Collagen type I is known as one of the main bone matrix molecules [27], and it can induce highly efficient cell adhesion of not only osteoblasts but also fibroblasts [28]. Indeed, both MC3T3-E1^{red} and NIH3T3^{green} could adhere to collagen type I under shear stress conditions (data not shown). We then considered that the reason why MC3T3-E1^{red} is superior in the adhesion competition on titanium discs under shear stress conditions

involves not only collagen type I, but also other factors. Collagen type I has rich binding sites for other adhesion molecules such as fibronectin [29]. Collagen type I is composed of three peptide chains and forms a higher-order structure. The titanium may make the conformation of collagen type I for osteoblast adhesion ideal. Further studies are needed to clarify this complex mechanism. NIH3T3^{Green} also expressed the collagen type I gene and fibronectin (Figure 3C). This suggests NIH3T3^{Green} may support MC3T3-E1^{Red} attachment.
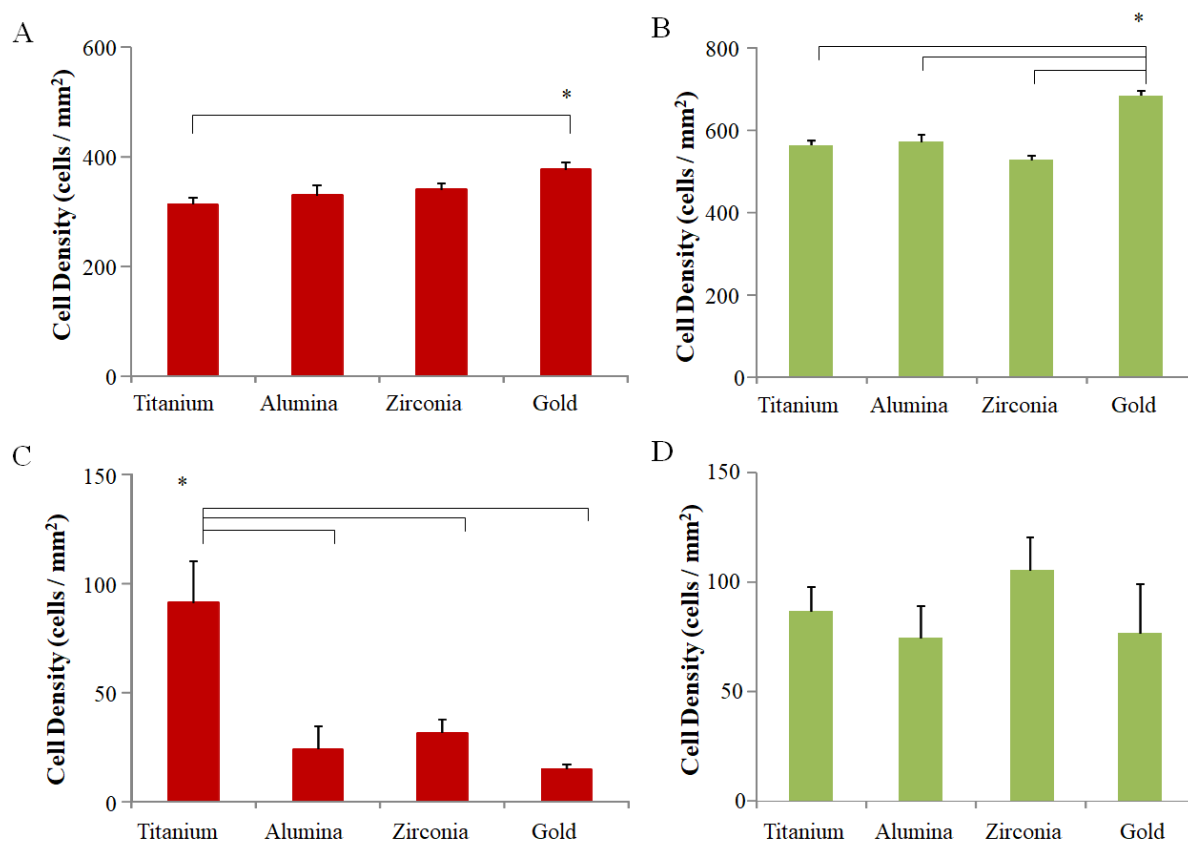
These results explain why using NIH3T3^{Green}-conditioned medium could promote MC3T3-E1^{Red} attachment on each disc (Figure 3A). The cell attachment number on titanium using the conditioned medium had similar results as using the medium containing FBS, which has multiple cell matrix molecules. The cell attachment number on the zirconia and alumina discs also increased. This result indicates that the fibroblast product matrix protein supports osteoblast attachment. However, the gene expression of collagen type I and fibronectin was not different between MC3T3-E1^{Red} and NIH3T3^{Green}, and so further study is required to clarify the difference in molecules. These results also suggest that new proteins produced from fibroblasts such as non-structured collagen may be important for osteoblasts. FBS also contains many non-cell adhesive proteins. The same cell attachment level on titanium was achieved using the FBS-containing medium and the conditioned medium, suggesting that titanium has a high potential for selectively absorbed matrix proteins; further experiments are required to clarify this.

After osteoblasts attach to the implantation surface, the next phase involves the differentiation of osteoprogenitor cells into osteoblasts and the mineralization of the extracellular matrix. We tested whether fibroblasts affect this differentiation. MC3T3-E1^{Red} and NIH3T3^{Green} were co-cultured and osteoblast

differentiation was investigated by ALP and Alizarin stain. MC3T3-E1^{Red} cultured on each disc could differentiate into ALP positive cells even when NIH3T3^{Green} and NIH3T3^{Green} were present. This seems to support MC3T3-E1^{red} differentiation. The low percentage of fibroblasts in the first cell mixture may promote osteogenic differentiation. On the other hand, calcium deposition stained by Alizarin Red S also seems to be promoted but with little contribution by NIH3T3^{Green}. These results suggest that fibroblasts may have a support role for osseointegration on titanium. Fibroblasts and osteoblasts compete for cell adhesion with each other on the surface of titanium and other materials such as alumina, zirconia, and gold. Fibroblasts were superior to osteoblasts in cell adhesion on the other materials and a fibroblast-rich environment is beneficial. As a consequence, in the second phase, fibrous tissues are incorporated into bone. In contrast to the other materials, osteoblasts are superior to fibroblasts in cell adhesion on titanium and fewer fibroblasts are required in this step. Therefore, bone can be formed without fibrous tissues and osseointegration can be achieved.

Supplement Figure 1

5. Conclusions

Although titanium has clinically been successful as an implant material for some time, this paper provides an explanation as to why titanium better promotes osseointegration than any of the other three materials were tested in our original competition co-culture model. This study suggests that the advantage of osteoblast attachment onto titanium might result in the best balance of osteoblasts and fibroblasts for osteogenesis on titanium compared to alumina, zirconia, and gold.

Acknowledgements

References

1. Gittens RA, Olivares-Navarrete R, Schwartz Z, Boyan BD. Implant osseointegration and the role of microroughness and nanostructures: lessons for spine implants. Acta biomaterialia 10 (2014): 3363-3371.

2. Wang IE, Shan J, Choi R, Oh S, Kepler CK, Chen FH, et al. Role of osteoblast-fibroblast interactions in the formation of the ligament-to-bone interface. J Orthop Res 25 (2007): 1609-1620.

3. Dohan Ehrenfest DM, Coelho PG, Kang BS, Sul YT, Albrektsson T. Classification of osseointegrated implant surfaces: materials, chemistry and topography. Trends Biotechnol 28 (2010): 198-206.

4. Albrektsson T, Zarb GA. Current interpretations of the osseointegrated response: clinical significance. Int J Prosthodont 6 (1993): 95-105.

5. Zheng Z, Ao X, Xie P, Wu J, Dong Y, Yu D, et al. Effects of novel non-thermal atmospheric plasma treatment of titanium on physical and biological improvements and in vivo osseointegration in rats. Scientific reports 10 (2020): 10637-10637.

6. Siddiqi A, Payne AGT, De Silva RK, Duncan WJ. Titanium allergy: could it affect dental implant integration?. Clin Oral Implants Res 22 (2011): 673-680.

7. Bijukumar DR, McGeehan C, Mathew MT. Regenerative Medicine Strategies in Biomedical Implants. Curr Osteoporos Rep 16 (2018): 236-245.

8. Liu X, Chu PK, Ding C. Surface modification of titanium, titanium alloys, and related materials for biomedical applications. Materials Science and Engineering: R: Reports 47 (2004): 49-121.

9. Bosshardt DD, Chappuis V, Buser D. Osseointegration of titanium, titanium alloy and zirconia dental implants: current knowledge and open questions. Periodontol 73 (2017): 22-40.

10. Wohlfahrt JC, Monjo M, Rønold HJ, Aass AM, Ellingsen JE, Lyngstadaas SP. Porous titanium granules promote bone healing and growth in rabbit tibia peri-implant osseous defects. Clin Oral Implants Res 21 (2010): 165-173.

11. Yamashita D, Machigashira M, Miyamoto M, Takeuchi H, Noguchi K, Izumi Y, et al. Effect of surface roughness on initial responses of osteoblast-like cells on two types of zirconia. Dent Mater J 28 (2009): 461-470.

12. Qu Z, Rausch-Fan X, Wieland M, Matejka M, Schedle A. The initial attachment and subsequent behavior regulation of osteoblasts by dental implant surface modification. J Biomed Mater Res A 82 (2007): 658-668.

13. Le Guehennec L, Lopez-Heredia MA, Enkel B, Weiss P, Amouriq Y, Layrolle P. Osteoblastic cell behaviour on different titanium implant surfaces. Acta Biomater 4 (2008): 535-543.

14. Hasegawa M, Saruta J, Hirota M, Taniyama T, Sugita Y, Kubo K, et al. A Newly Created Meso-, Micro-, and Nano-Scale Rough Titanium Surface Promotes Bone-Implant Integration. Int J Mol Sci 21 (2020).

15. Ananth H, Kundapur V, Mohammed HS, Anand M, Amarnath GS, Mankar S. A Review on

Biomaterials in Dental Implantology. Int J Biomed Sci 11 (2015): 113-120.

16. Ryu JY, Siswanto A, Harimoto K, Tagawa Y. Chimeric analysis of EGFP and DsRed2 transgenic mice demonstrates polyclonal maintenance of pancreatic acini, Transgenic Res 22 (2013): 549-556.

17. Harimoto K, Yoshida Y, Yoshihara K, Nagaoka N, Matsumoto T, Tagawa Y. Osteoblast compatibility of materials depends on serum protein absorbability in osteogenesis. Dental Materials Journal 31 (2012): 674-680.

18. Tamai M, Yamashita A, Tagawa Y. Mitochondrial development of the in vitro hepatic organogenesis model with simultaneous cardiac mesoderm differentiation from murine induced pluripotent stem cells. J Biosci Bioeng 112 (2011): 495-500.

19. Cai K, Müller M, Bossert J, Rechtenbach A, Jandt KD. Surface structure and composition of flat titanium thin films as a function of film thickness and evaporation rate. Applied Surface Science 250 (2005): 252-267.

20. Jäger M, Zilkens C, Zanger K, Krauspe R. Significance of nano- and microtopography for cell-surface interactions in orthopaedic implants, J Biomed Biotechnol 2007 (2007): 69036.

21. Guida L, Oliva A, Basile MA, Giordano M, Nastri L, Annunziata M. Human gingival fibroblast functions are stimulated by oxidized nano-structured titanium surfaces. J Dent 41 (2013): 900-907.

22. Schultze-Mosgau S, Blatz MB, Wehrhan F, Schlegel KA, Thorwart, Holst S. Principles and mechanisms of peri-implant soft tissue healing. Quintessence Int 36 (2005): 759-769.

23. Geurs NC, Vassilopoulos PJ, Reddy MS. Soft tissue considerations in implant site development. Oral Maxillofac Surg Clin North Am 22 (2010): 387-405.

24. Huang X, Das R, Patel A, Nguyen TD. Physical Stimulations for Bone and Cartilage Regeneration. Regen Eng Transl Med 4 (2018): 216-237.

25. Kapur S, Baylink DJ, Lau KH. Fluid flow shear stress stimulates human osteoblast proliferation and differentiation through multiple interacting and competing signal transduction pathways. Bone 32 (2003): 241-251.

26. Ban Y, Wu YY, Yu T, Geng N, Wang YY, Liu XG, et al. Response of osteoblasts to low fluid shear stress is time dependent. Tissue Cell 43 (2011): 311-317.

27. Filippi M, Born G, Chaaban M, Scherberich A. Natural Polymeric Scaffolds in Bone Regeneration. Front Bioeng Biotechnol 8 (2020): 474-474.

28. Anselme K. Osteoblast adhesion on biomaterials, Biomaterials 21 (2000): 667-681.

29. Gullberg D, Gehlsen KR, Turner DC, Ahlén K, Zijenah LS, Barnes MJ, et al. Analysis of alpha 1 beta 1, alpha 2 beta 1 and alpha 3 beta 1 integrins in cell-- collagen interactions: identification of conformation dependent alpha 1 beta 1 binding sites in collagen type I. Embo j 11 (1992): 3865-3873.